J. Phycol. **43,** 156–170 (2007)

DOI: 10.1111/j.1529-8817.2006.00305.x

DIVERSITY IN THE GENUS *SKELETONEMA* (BACILLARIOPHYCEAE): III. PHYLOGENETIC POSITION AND MORPHOLOGICAL VARIABILITY OF *SKELETONEMA COSTATUM* AND *SKELETONEMA GREVILLEI*, WITH THE DESCRIPTION OF *SKELETONEMA ARDENS* SP. NOV.[1]

Diana Sarno[2], *Wiebe H. C. F. Kooistra, Sergio Balzano*

Stazione Zoologica Anton Dohrn, Villa Comunale, 80121 Naples, Italy

Paul E. Hargraves

Graduate School of Oceanography, University of Rhode Island, Narragansett, Rhode Island 02882-1197, USA

and

Adriana Zingone

Stazione Zoologica Anton Dohrn, Villa Comunale, 80121 Naples, Italy

***Skeletonema costatum* (Grev.) Cleve emend. Zingone et Sarno and *S. grevillei* Sarno et Zingone were known only from the type material collected from Hong Kong waters more than a century ago. Both species have now been collected as live material, and their morphology and phylogenetic position are investigated in this study. Eight *Skeletonema* strains isolated from Florida, USA; Uruguay; and Brazil are attributed to *S. costatum*, while one strain from Oman is ascribed to *S. grevillei* based on morphological similarity to the type material of these species. In addition, a new *Skeletonema* species, *S. ardens* Sarno et Zingone, is described for a strain from Singapore and two from northern Australian waters. *Skeletonema ardens* has terminal fultoportula processes ending in a tapered, undulate protrusion and long intercalary fultoportulae with 1:1 junctions. The rimoportula of terminal valves is located at the margin of the valve face. No major morphological variations were observed within *S. grevillei* and *S. ardens* along a salinity gradient, whereas in *S. costatum*, the processes shortened and the valves came into close contact at low salinities, as already described for *S. subsalsum* (Cleve) Bethge. Consistent with their morphology, *Skeletonema costatum* and Skeletonema subsalsum also had similar rDNA sequences. *Skeletonema grevillei* and *S. ardens* were distinct in the large subunit (LSU) phylogeny. *Skeletonema ardens* exhibited consistent intraspecific genetic differences in both the LSU and small subunit (SSU) rDNA.**

Key index words: **diatoms; LSU rDNA; morphology; phylogeny; salinity; *Skeletonema ardens*; *Skeletonema costatum*; *Skeletonema grevillei*; SSU rDNA**

Abbreviations: **CCAP, Culture Collection of Algae and Protozoa; CCMP, the Provasoli-Guillard National Center for Cultures of Marine Phytoplankton; CSIRO, Commonwealth Scientific and Industrial Research Organisation; FPP, fultoportula process; GTR, general time reversible; IFPP, intercalary fultoportula process; IRP, intercalary rimoportula; IRPP, intercalary rimoportula process; ML, maximum likelihood; MP, maximum parsimony; NJ, neighbor joining; RELL, resampling of estimated ln likelihood; SZN, Stazione Zoologica A. Dohrn of Naples; TFPP, terminal fultoportula process; TRP, terminal rimoportula; TRPP, terminal rimoportula process**

The centric diatom *Skeletonema costatum* has long been considered one of the most conspicuous and widespread members of the coastal marine phytoplankton. Recently, it was discovered that a number of distinct species were included under this name (Sarno et al. 2005). *Skeletonema costatum* was originally described by Greville (1866) as *Melosira costata*, based on light microscopy (LM) of material from Hong Kong Bay (Zingone et al. 2005). LM and EM examination of the original material revealed the presence of two *Skeletonema* species with a markedly distinct frustule ultrastructure. By comparison with the original drawings (Greville 1866), one was identified as *S. costatum sensu stricto*. Morphological analyses showed that it has a unique combination of ultrastructural features, including flattened and closed tubular processes emerging from the fultoportulae of the intercalary valves (intercalary fultoportula processes, IFPPs), open terminal valve fultoportula processes (terminal fultoportula processes, TFPPs), asymmetrical 1:2 junctions between sibling valves, and marginal terminal rimoportulae (TRPs) (Zingone et al. 2005). The other morph required the establishment of a new species, *S. grevillei* Sarno et Zingone, differing from *S. costatum* by having open IFPPs that mostly connect to adjacent cells with

[1]Received 10 April 2006. Accepted 2 November 2006.
[2]Author for correspondence: e-mail diana@szn.it.

1:1 junctions. A unique feature of *S. grevillei* is the presence of silica bridges joining the basal parts of the fultoportula processes (FPPs). Like *S. costatum*, this species has marginal terminal rimoportulae.

After the establishment of *S. costatum* by Greville (1866), at least four other species were validly described, namely *S. tropicum* Cleve, *S. subsalsum* (Cleve) Bethge, *S. potamos* (Weber) Hasle, and *S. menzelii* Guillard, E. J. Carp. et Reimann. Yet, notably, neither *S. costatum sensu stricto* nor *S. grevillei* were ever observed or illustrated again, nor were they among the taxa examined by Medlin et al. (1991). The latter described *S. pseudocostatum* as distinct from what they believed to be *S. costatum*, based on morphology and small subunit (SSU) rDNA sequences. Sarno et al. (2005) examined large subunit (LSU) and SSU rDNA sequences and morphological traits of 35 *Skeletonema* strains, recognizing four new species (*S. dohrnii* Sarno et Kooistra, *S. grethae* Zingone et Sarno, *S. japonicum* Zingone et Sarno, and *S. marinoi* Sarno et Zingone), but neither *S. costatum* nor *S. grevillei* were found. Zingone et al. (2005) only had access to fixed material of *S. costatum* and *S. grevillei* from a net sample obtained from a single site, and the lack of further samples or cultured strains constrained the documentation of morphological variability of the two species, while their phylogenetic position was inferred from their ultrastructural characteristics. During the course of a study on the global biodiversity and biogeography of the genus *Skeletonema*, a number of strains closely resembling *S. costatum* and *S. grevillei* were collected, allowing more detailed morphological analysis of these species (Kooistra et al., submitted). In addition, three strains showing ultrastructural features that were not previously encountered are described as a new species: *S. ardens*. The phylogenetic positions of the three taxa are inferred from their LSU and SSU rDNA sequences and discussed alongside the characters that are thought to be phylogenetically informative in *Skeletonema*.

MATERIALS AND METHODS

Isolation of strains and culture conditions. Cultures of the strains SZN B202 and SZN B203 were established by micropipette isolation of single colonies from a mixed net sample collected in the Indian River Lagoon, FL, USA (Table 1). Other strains of *S. costatum* were isolated in the same way from Montevideo (Uruguay) samples provided by Silvia Mendez. Strains from the Lagoa dos Patos (Brazil) were provided by Dr. Marli Bergesch. The strains of *S. grevillei* and *S. ardens* were obtained from the Provasoli-Guillard National Center for Cultures of Marine Phytoplankton (CCMP; Bigelow, USA) and from the Commonwealth Scientific and Industrial Research Organisation (CSIRO) culture collection (Hobart, Australia).

All cultures were maintained at the Stazione Zoologica Anton Dohrn, Naples (SZN), in f/2 medium, adjusted to a salinity of 36 psu. Cultures were kept in glass tubes at temperatures ranging from 15°C to 22°C and a 12:12 light:dark (L:D) cycle at 100 μmol photons $\cdot m^{-2} \cdot s^{-1}$ emitted from cool-white fluorescent tubes.

Morphological variability of Skeletonema *species in relation to salinity.* The growth of *S. costatum* (strains SZN B202 and SZN B211), *S. grevillei* (strains CCMP794 and CS347), and *S. ardens* (strain CCMP1685) was monitored at salinities between 0 and 35 psu. Media with different salinities were prepared with f/2 and Erd-Schreiber medium in different proportions. To adapt strains to different salinities, minute amounts of cultures were transferred every third day to media with a salinity of 2.5 psu higher or lower than the one in which they were growing. Exponentially growing cultures of each strain were observed with LM and EM at their optimal, minimum, and maximum salinity tolerance values.

Light microscopy. Light microscope observations were made on exponentially growing cultures or natural samples with a Zeiss Axiophot microscope (Carl Zeiss, Oberkochen, Germany) equipped with Nomarski differential interference contrast (DIC), phase contrast, and bright-field optics. Light micrographs were taken using a Zeiss Axiocam digital camera. To remove organic matter, samples from cultures or field material were treated with acids (1:1:4, sample:HNO_3:H_2SO_4), boiled for a few seconds, and then washed with distilled water. Permanent slides were prepared by mounting the dry, clean material in Hyrax (Custom Research and Development, Auburn, CA, USA; Hasle 1978).

Electron microscopy. Acid-cleaned material was mounted on stubs, sputter coated with gold-palladium, and observed using a Philips 505 SEM (Philips Electron optics BV, Eindhoven, the Netherlands), or mounted on Formvar-coated grids (Agar Scientific, Stanstead, Essex, UK) and observed using a Philips 400 TEM. Fixed samples not subjected to cleaning were dehydrated in an ethanol series, critical point dried substituting 100% ethanol with CO_2, sputter coated with gold-palladium, and observed with SEM.

The terminology used to describe ultrastructural features of *Skeletonema* species follows Anonymous (1975) and Ross et al. (1979), while rimoportulae, fultoportulae, and their processes are named as in Sarno et al. (2005).

DNA extraction, PCR amplification, sequencing, and phylogenetic analyses. For molecular analysis, cultures of *Skeletonema* species were harvested during the exponential growth phase by filtration on 0.45 μm pore-size polycarbonate filters. DNA extraction and purification were performed as in Kooistra et al. (2003). PCR amplification of the nuclear-encoded SSU rDNA was carried out as described in Kooistra et al. (2003); PCR products were sequenced with forward primers 1F 5′-AACCTGGTTGATCCTGCCAGT-3′, 528F 5′-CGGTAATTCCAGCTCC-3′, and 1055F 5′-GGTGGTGCATGGCCG-3′; and reverse primers 1528R 5′-TGATCCTTCTGCAGGTTCACCTAC-3′, 1055R 5′-CGGCCATGCACCACC-3′, and 690R 5′-AGAATTTCACCTCTG-3′. The PCR amplification of the nuclear-encoded LSU rDNA was carried out as in Orsini et al. (2002), and products were sequenced using the same primers. Sequence reactions were obtained with BigDye Terminator Cycle Sequencing technology (Applied Biosystems, Foster City, CA, USA) and purified in automation using a robotic station "Biomek FX" (Beckman Coulter, Fullerton, CA, USA). Products were analyzed on an Automated Capillary Electrophoresis Sequencer "3730 DNA Analyzer" (Applied Biosystems). Sequences were aligned using the program Multalin (Corpet 1998) and then adjusted by eyeball in the sequence alignment editor Se-Al version 2.0a11 (Rambaut 1996–2002).

The strains used in the molecular analyses are listed in Table 1, together with the GenBank accession numbers of their SSU rDNA and partial LSU rDNA regions. Complete alignments are available upon request from Wiebe Kooistra. Before phylogenetic analysis, we removed the positions of the PCR primers and positions showing a gap in all but one of the sequences.

TABLE 1. List of *Skeletonema* strains used in this study, with their names, strain IDs, geographic origin, and GenBank numbers of their partial LSU rDNA sequences.

Strain ID	Geographic origin	Ocean	Collection dd/mm/yy	GenBank LSU rDNA	GenBank SSU rDNA
Skeletonema ardens Sarno et Zingone (Sarno et al., this study)					
CCMP794	Singapore	NEI	–/12/73	DQ396492	DQ396520
CS347	Gulf of Carpentaria, Australia	SWP	–/–/91	DQ396493	DQ396521
CS348	Gulf of Carpentaria, Australia	SWP	–/–/91	DQ396494	DQ396522
S. costatum (Grev.) Cleve emend. Zingone et Sarno (Zingone et al. 2005)					
SZN B202	Indian River Lagoon, FL, USA	NWA	28/01/03	DQ396489	
SZN B203	Indian River Lagoon, FL, USA	NWA	28/01/03	DQ396490	DQ396524
SZN B206	Montevideo, Uruguay	SWA	29/03/04	DQ396491	
SZN B207	Montevideo, Uruguay	SWA	29/03/04	DQ396491	
SZN B211	Montevideo, Uruguay	SWA	29/03/04	DQ396491	DQ396523
SZN B212	Montevideo, Uruguay	SWA	29/03/04	DQ396491	
B	Museu, Lagoa dos Patos, Brazil	SWA	29/10/04	DQ396491	
C	Museu, Lagoa dos Patos, Brazil	SWA	29/10/04	DQ396491	
S. dohrnii Sarno et Kooistra (Sarno et al. 2005)					
SZN B104 CCMP2479	GON, Italy	MED	04/02/02	AJ633537	AJ632210
S. grethae Zingone et Sarno (Sarno et al. 2005)					
CCMP780	Eel Pond, Woods Hole, MS, USA	NWA	–/–/74	AJ633522	AJ632205
CCAP1077/3	Narragansett Bay, USA	NWA	–/10/86	AJ633521	AJ632204
S. grevillei Sarno et Zingone (Zingone et al. 2005)					
CCMP1685	23.6500 N 58.7000 E Arabian Sea, Muscat, Oman	NWI	Autumn 93	DQ396495	DQ396512
S. japonicum Zingone et Sarno (Sarno et al. 2005)					
SZN B149 CCMP2506	Hiroshima Bay, Seto Inland Sea, Japan	NWP	01/10/02	AJ633524	As CCMP784
CCMP784	Uncle Sam Bank, Baja California, Mexico	NEP	–/10/65	AJ633524	DQ396518
CCMP1281	South California Bight, near Santa Cruz Island; California, USA	NEP	Winter 90	AJ633524	AY485473
UBC-18/C	Georgia Strait, USA	NEP	?	AJ633524	M54988.1
S. marinoi Sarno et Zingone (Sarno et al. 2005)					
CCMP1009	39.2000 N 69.3333 W continental slope, (USA)	NWA	–/–/77	AJ633536	AJ535165
S. menzelii Guillard, E. J. Carpenter et Reimann (Guillard et al. 1974)					
SZN B82	GON, Italy	MED	18/12/01	AJ633526	AJ632217
SZN B83	GON, Italy	MED	18/12/01	AJ633525	AJ632218
CCMP787	32.1667 N 64.5000 W Sargasso Sea	NWA	22/05/59	AJ633527	AJ536450
CCMP790	Chase Creek, Dennis, MA, USA	NWA	–/09/79	AJ633528	AJ535168
TAGIRI-11	Tagiri site, off Fukuyama, Kagoshima Bay, Japan	NWP			AB191419
S. pseudocostatum Medlin emend. Zingone et Sarno (Sarno et al. 2005)					
SZN B77 CCMP2472	GON, Italy	MED	29/05/01	AJ633507	AJ632207
S. subsalsum (Cleve) Bethge (Bethge 1928)					
CCAP1077/8	Lower Lough Erne, Co. Fermanagh, Northern Ireland, UK	NEA	–/–/91	AJ633539	AJ535166
S. tropicum Cleve (Cleve 1900)					
SZN M98	GON, Italy	MED	14/04/04	DQ396499	DQ396513
SZN M99	GON, Italy	MED	14/04/04	DQ396499	DQ396514
CCMP788	Galveston Channel, TX, USA	NWA	–/–/73	AJ633520	
SZN B205	Montevideo, Uruguay	SWA	29/03/04	DQ396501	DQ396515
SZN B210	Montevideo, Uruguay	SWA	29/03/04	As SZN B208	DQ396516
CCMP2070	Perlas Islands, Gulf of Panama	NEP	01/03/97	DQ400577	DQ396517

"–" in the collection date signifies collection date unknown. GON, Gulf of Naples; LSU, large subunit; MED Mediterranean Sea; NEA, northeastern Atlantic Ocean; NEI, northeastern Indian Ocean; NEP, northeastern Pacific Ocean; NWA, northwestern Atlantic Ocean; NWI, northwestern Indian Ocean; NWP, northwestern Pacific Ocean; SSU, small subunit; SWA, southwestern Atlantic Ocean; SWP, southwestern Pacific Ocean.

The SSU rDNA alignment included 26 *Skeletonema* sequences (the ingroup), of which the following were new: all three *S. ardens*, both *S. costatum*, *S. grevillei*, all five *S. tropicum*, one from an environmental sample (TAGIRI-11), and three out of four *S. japonicum*. The GenBank sequence of UBC 18/C, for which we have no morphological data, was reported as *S. grethae* in Sarno et al. (2005), but was recovered among those of *S. japonicum* in the present study and in Alverson and

TABLE 2. Main morphological characters distinguishing *Skeletonema* species.

Species	Chloroplasts	Satellite pores	TFPP Shape	TFPP Tip width	TFPP Tip shape	IFPP joints[a]	TRP position	IRP	Cingular band ultrastructure
Skeletonema ardens	1–2	3	Split tube	Narrow	Spiny	1:1	Marginal	Short	Hyaline areas
S. costatum	1–2	3	Close with a pore	Narrow	Clawlike	1:2	Marginal	Long	Rows of pores
S. dohrnii	1–2	3	Split tube	Flared	Dentate	1:2	Central	Short	Hyaline areas
S. grethae	1–2	3	Split tube	Narrow	Clawlike, truncated, or spiny	1:1	Central	Short	Hyaline areas
S. grevillei	1–2	3	Split tube	Narrow	Truncated or spiny	1:1	Marginal	Short	Hyaline areas
S. japonicum	1–4	3	Close at the base	Narrow	Truncated or clawlike	1:2	Central	Short	Rows of pores
S. marinoi	1–2	3	Split tube	Flared	Dentate	1:2	Central	Short	Rows of pores
S. menzelii	1–2	2	Split tube	Narrow	Spiny	-	Central		Hyaline areas
S. pseudocostatum	1–2	3	Close at the base	Narrow	Clawlike, truncated, or spiny	1:1	Central	Short	Hyaline areas
S. subsalsum	1–2	3	Close with a pore	Narrow	Hooklike	1:2	Central	Long	Rows of pores
S. tropicum	1–7	3	Split tube	Narrow	Clawlike or truncated	1:2	Central	Short	Rows of pores

[a] 1:2 includes only cases when 1:2 connections are found in contiguous junctions. All species forming 1:1 connections can occasionally form isolated 1:2 joints.

IFPP, intercalary fultoportula process; IRP, intercalary rimoportula; TFPP, terminal fultoportula process; TRP, terminal rimoportula.

Kolnick (2005). Nine sequences in Thalassiosirales were chosen as the near-outgroup, and four in Lithodesmiales (*sensu* Medlin and Kaczmarska 2004) as the distant-outgroup. Only four gaps were needed among the *Skeletonema* sequences, whereas alignment with the outgroup sequences needed 18 more gaps in the ingroup sequences without altering their alignment. Fifteen positions were removed from the subsequent analyses because they each showed a gap in all but one sequence. Sequences of *S. tropicum* strains M98 and M99 showed an ~300 base pairs insertion in the position of primer 1528R (5′-GTAGG-insert-TGAACCTGCAGAAGGATCA-3′ indicated in the forward direction), but this insert did not affect tree reconstruction because the positions of terminal primers were removed before analyses.

The LSU rDNA alignment included 31 *Skeletonema* sequences (the ingroup), of which the following were new: all eight of *S. costatum*, the one of *S. grevillei*, all three of *S. ardens*, two of three of *S. japonicum*, and five of six of *S. tropicum*. We included nine sequences of other Thalassiosirales as near-outgroups, and three Lithodesmialean sequences as far-outgroups. Although the LSU region was sequenced from the forward primer DIR to the reverse primer D3Ca, we eliminated all positions to the 3′-end of position 603 because several near-outgroup sequences were available only until that point, and the ingroup showed only a few variable sites beyond that position.

Phylogenetic analyses were carried out in PAUP* version 4.0b10 (Swofford 2002). The phylogenetic signal in the ingroup was explored by comparing the value of skewedness of 100.000 random trees option in PAUP* against threshold values in Hillis and Huelsenbeck (1992). Maximum-parsimony (MP) analyses were performed using heuristic searches with tree-bisection-reconnection branch swapping. Branches were collapsed if their minimum length was 0; ambiguities were treated as polymorphisms, and gaps as missing data. The MP-bootstrap values (1000 replicates) were calculated using the same settings. Before maximum-likelihood (ML) analyses, we eliminated sequences that were identical to others, until single representatives remained. Heuristic searches in ML were constrained with a general time-reversible (GTR) base substitution model. The various substitution rates, base frequencies, proportion of invariable sites, and the shape parameter assuming a γ distribution of positional rate variation were estimated given the data set, and a neighbor-joining (NJ) tree inferred from pair-wise Jukes-Cantor distances among the sequences. Bootstrap values associated with internodes (1000 replicates) were calculated using NJ of pair-wise ML-distance values constrained using the same model, but this shortcut was only taken if an NJ tree inferred from pair-wise ML distances did not have a significantly worse –ln likelihood than the ML tree. The –ln likelihood values of alternative tree topologies were tested against those of the best one using the Shimodaira-Hasegawa topology test in PAUP* [resampling of estimated ln likelihood (RELL) using 1000 replicates].

RESULTS

Three distinct morphs were identified, two of which corresponded to the morphology of the type material of *S. costatum* and *S. grevillei*, and one that constituted a new species. The morphological characteristics of the three species examined are summarized in Table 2, together with those of other known *Skeletonema* species (Sarno et al. 2005).

Skeletonema costatum *(Greville) Cleve emend. Zingone et Sarno (Fig. 1, A–J). Material examined*: Strains SZN B202, SZN B203, SZN B206, SZN B207, SZN B211, SZN B212, B, and C (see Table 1 for explanation of strain identifications).

Cells form long chains (up to 60 cells) and have a valve diameter of 8–12 μm. Each cell contains 1–2 chloroplasts (Fig. 1A). The TFPPs are split tubes throughout, with a narrow distal part ending in a clawlike protrusion (Fig. 1, B–D). The IFPPs are flattened tubes, with an external hole at their base and a longitudinal suture running from the hole toward the process end (Fig. 1, E–F). In cultured

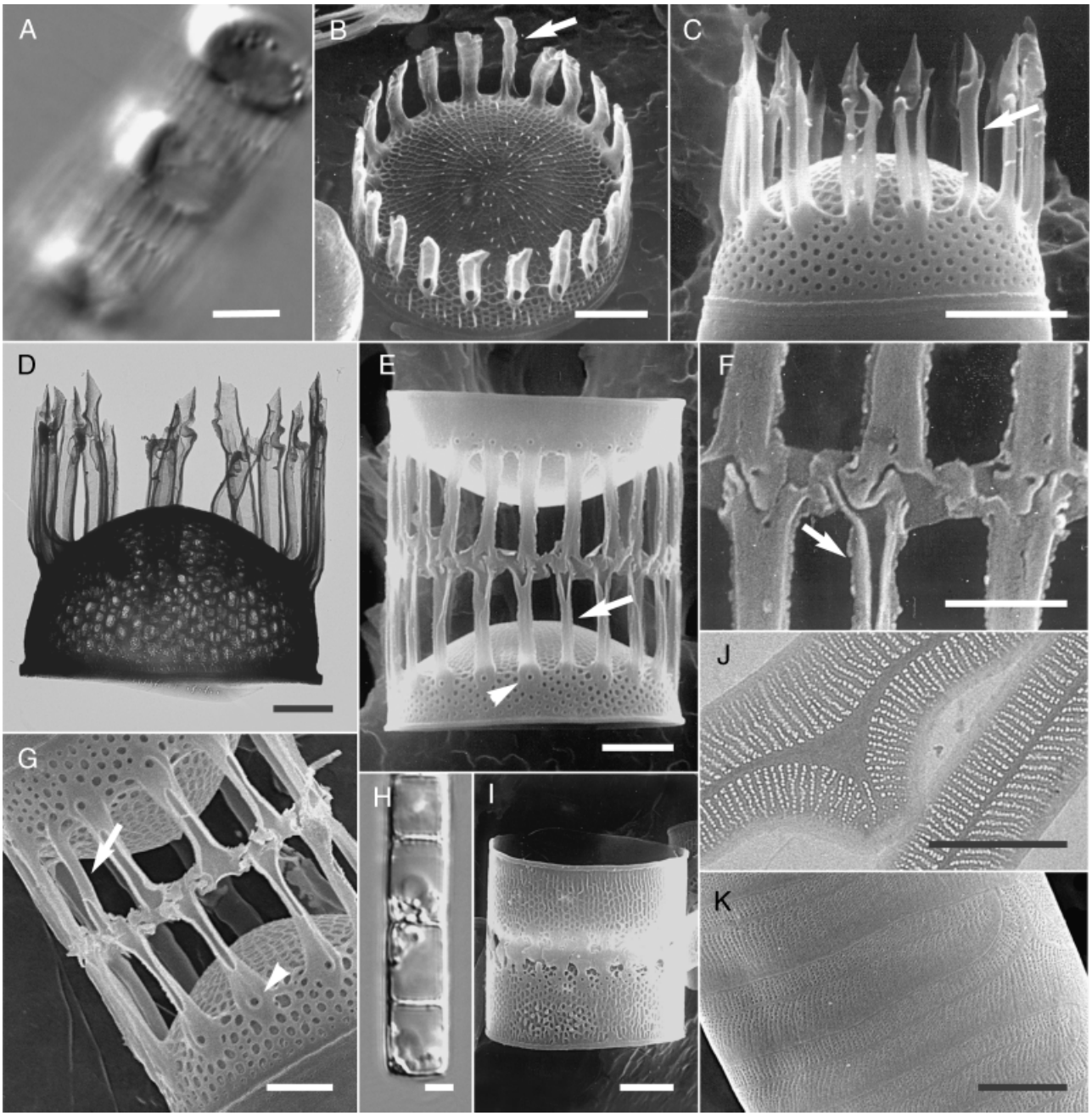

Fig. 1. *Skeletonema costatum*. LM, differential interference contrast: A, H. SEM: B, C, E, F, G, I, and K. TEM: D and J. (A) Strain SZN B202, intercalary cells of a colony showing the 1:2 IFPP connection and the zigzag line at the junction. Scale bar, 10 µm. (B) Strain SZN B202, terminal valve with TRPP in the marginal position (arrow). Scale bar, 2 µm. (C) Strain SZN B202, terminal valve, with claw-shaped TFPP tips and the marginal TRPP (arrow). Scale bar, 2 µm. (D) Strain SZN B211, terminal valve. Scale bar, 1 µm. (E) Strain SZN B202, intercalary valves of a colony with 1:2 IFPP junctions. Note the flattened and closed IFPPs, with an external pore at their base (arrowhead) and the long IRPP connected to two IFPPs (arrow). Scale bar, 2 µm. (F) Strain SZN B202 grown at 10 psu, detail of 1:2 junction also including the IRPP (arrow). Scale bar, 1 µm. (G) Strain SZN B211, intercalary valves with IFPPs open for almost their whole length and the external pore at their base (arrowhead). Note the long IRPP (arrow) connected to two IFPPs. Scale bar, 1 µm. (H) Strain SZN B202 grown at 1 psu, part of a colony with appressed valves. Scale bar, 5 µm. (I) Strain SZN B202 grown at 1 psu, two intercalary valves with high mantles and extremely short processes. Scale bar, 2 µm. (J) Strain C, cingular bands with rows of small pores. Scale bar, 1 µm. (K) Strain SZN B211, detail of a cingulum. Scale bar, 1 µm. IFPP, intercalary fultoportula process; IRPP, intercalary rimoportula process; LM, light microscopy; TFPP, terminal fultoportula process; TRPP, terminal rimoportula process.

material, the suture is frequently open distally or even along the whole length of the process (Fig. 1G). Each IFPP generally connects to two IFPPs of the next valve (1:2 junction), resulting in a zigzag appearance of the junction in LM. The configuration of opposite IFPPs of sibling valves varies from completely displaced (Fig.

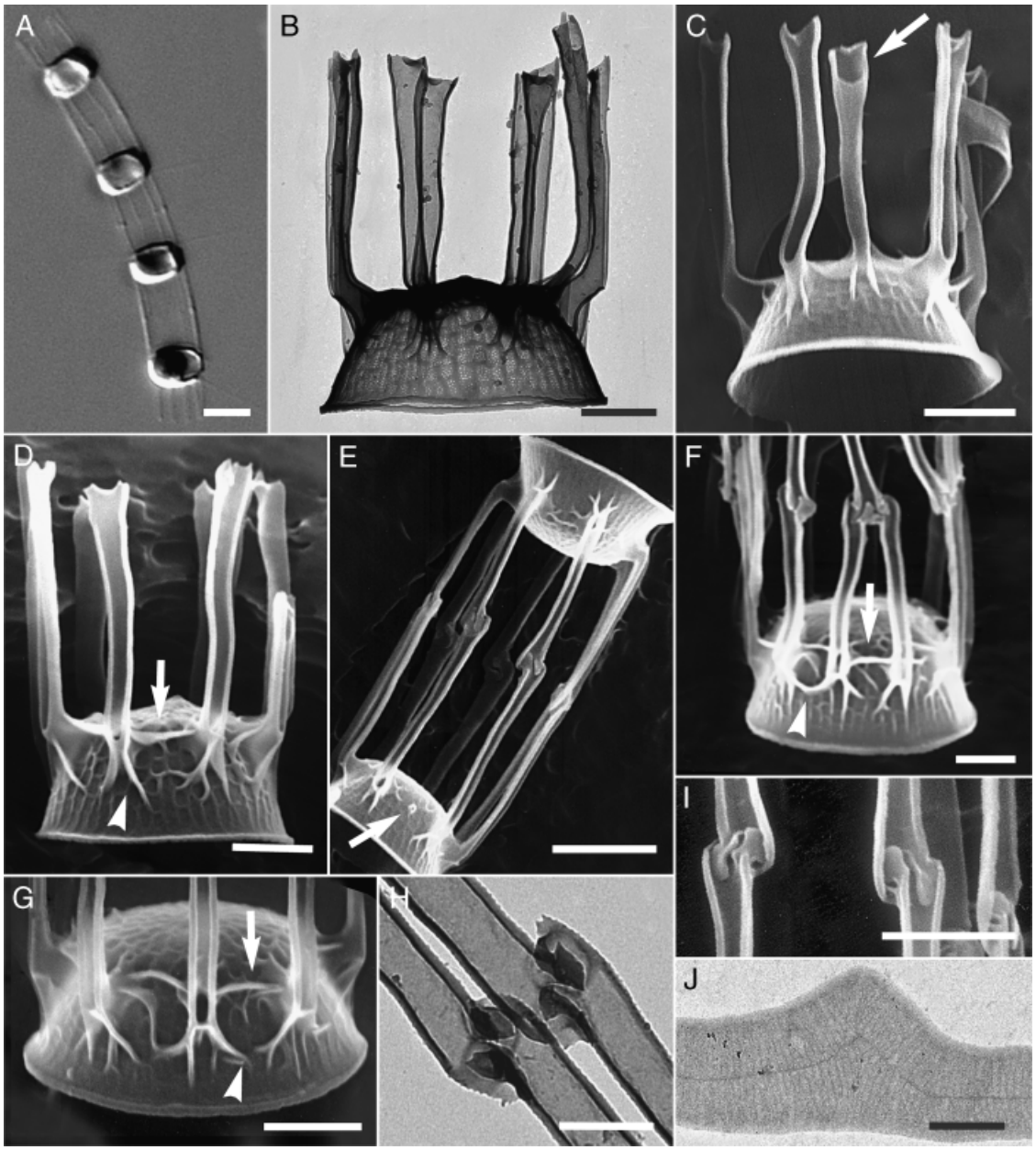

FIG. 2. *Skeletonema grevillei*. LM, differential interference contrast: A. SEM: C–G and I. TEM: B, H, and J. (A) Strain SCX09 (Xiamen Harbour, China), colony. Scale bar, 5 µm. (B) Strain CCMP1685, terminal valve of a colony with truncated TFPPs. Scale bar, 1 µm. (C) Strain CCMP1685, terminal valve showing the long marginal TRPP with the obliquely truncated tip margin (arrow). Scale bar, 1 µm. (D) Strain CCMP1685, terminal valve with TFPP tips showing lateral spines; note the ridges connecting the internal face of the FPP bases among them (arrow) and to the valve mantle (arrowhead). Scale bar, 1 µm. (E) Strain CCMP1685, intercalary valves with 1:1 IFPP junctions and short IRPP (arrow). Scale bar, 2 µm. (F) Strain CCMP1685, detail of an intercalary valve with a single 1:2 connection to the sibling cell; siliceous ridges connect the internal face (arrow) and the lateral faces (arrowhead) of FPP bases. Scale bar, 1 µm. (G) Strain CCMP1685, detail of a valve with ridges connecting the internal face (arrow) and the lateral faces (arrowhead) of the FPP bases. Scale bar, 1 µm. (H) Strain CCMP1685, detail of two 1:1 junctions. Scale bar, 0.5 µm. (I) Strain CCMP1685, detail of 1:1 connections with forklike joints. Scale bar, 1 µm. (J) Strain CCMP1685, cingular band with thin transverse ribs interspaced by hyaline areas. Scale bar, 1 µm. FPP, fultoportula process; IFPP, intercalary fultoportula process; IRPP, intercalary rimoportula process; LM, light microscopy; TFPP, terminal fultoportula process; TRPP, terminal rimoportula process.

1G) to almost aligned (Fig. 1E), with slightly asymmetrical lateral expansion of process tips. When processes are almost aligned (Fig. 1, E–F), one process may be connected to only one process of the opposite valve, while the lateral expansions of its tip join those of contiguous processes of the same valve. In all cases, a continuous line is evident at the level of the junctions. In each intercalary and terminal valve, a rimoportula with a relatively long external process is located near the valve margin and substitutes for one of the fulto-

portulae (Fig. 1, B, C, E, and G). The process of the intermediate rimoportula (IRPP) joins two IFPPs of the sibling valve (Fig. 1, E and G), while the process of the terminal rimoportula (TRPP) has a spoutlike teapot end (Fig. 1C). The copulae have a central longitudinal ridge and transverse branching ribs that are interspaced by rows of small pores (Fig. 1, J and K).

Strain B202 grew actively between 0 and 35 psu, while strain B211 grew between 3 and 35 psu. The FPPs and the rimoportula process were extremely reduced at salinities below 3 psu, whereas at 1 psu, FPPs were not discernible in LM, and the sibling valves came into close contact (Fig. 1H). With SEM, extremely short, intricately intertwined IFPPs were observed, and valves had a very deep mantle and almost flat valve faces (Fig. 1I).

Skeletonema grevillei *Sarno et Zingone (Fig. 2, A–J). Material examined:* Strain CCMP1685. Cells are 3–4 μm in diameter and form short colonies (as many as seven cells). Each cell contains one or two chloroplasts (Fig. 2A). The FPPs are open along their entire length in both terminal and intercalary valves (Fig. 2, B–G). The TFPPs are irregularly truncated at their tips, which bear one or two small lateral spines (Fig. 2, B–D). The distal ends of the IFPPs are narrow and connect to those of the adjacent valve in a 1:1 fashion (Fig. 2E) by a thickened fork- or knucklelike joint (Fig. 2, E, H, and I). Occasionally, one process joins two opposite processes (Fig. 2F). Siliceous ridges link the IFPP bases to each other and to the valve mantle (Fig. 2, D, F, and G). The ridges may be extremely reduced or even lacking in some specimens. The rimoportula lies close to the valve face margin near the marginal ring of FPPs. The intercalary rimoportula (IRP) opens externally with a small tubule (Fig. 2E), whereas the TRPP is as long as the TFPPs and ends with an irregularly truncated edge (Fig. 2C). The copulae are very delicate, with a median ridge running along their whole length. The ridge is flanked by thin, transverse branching ribs, interspersed with a hyaline area (Fig. 2J).

Skeletonema grevillei did not show significant morphological variation when grown at salinities between 10 and 35 psu, the range permitting growth. Short IFPPs were frequently observed in cultures grown at salinities immediately above the lowest salinity tolerated by this strain.

Skeletonema ardens *Sarno et Zingone sp. nov. (Fig. 3, A–K).* Cellulae catenas breves formantes. Valvae diameter 2–6 μm longus. In quaque cellula 1–2 chloroplasti. Tubuli externi fultoportularum divisi. Partes extremae tubulorum ut ungues vel ut flamma in valvis terminalibus catenae. Tubulus quisque iunctus est cum tubulo valvae sororis. Rimoportula iuxta marginem in valvis intercalaribus et in valvis terminalibus catenae posita est. Tubulus externus rimoportulae brevis in valvis intercalaribus, longus in valvis terminalibus catenae. Teniae costis transversis et areis hyalinis interpositis praeditae sunt.

Cells in relatively short chains. The valve diameter is 2–6 μm. Each cell contains one to two chloroplasts. External processes of the fultoportulae split, ending in a thin, undulate spine in terminal valves. In intermediate cells, each process connects to a process of the sibling valve. The rimoportula lies close to the valve face margin in both intercalary and terminal valves. The rimoportula process is short in intercalary valves, and long in terminal valves. The copulae have transverse ribs interspersed by hyaline areas.

Holotype: A permanent slide of strain CS347 has been deposited in the SZN Museum as number SZN CS347.

Iconotype: Figure 3, A–K.

Material examined: Strains CS347, CS348, and CCMP794.

Type locality: Gulf of Carpentaria, Australia.

Etymology: The epithet *ardens* (burning) refers to the shape of the tip of the terminal fultoportula processes.

Description: Cells are 2–6 μm in diameter, solitary or forming relatively short chains (18 cells maximum) (Fig. 3, A and B). Strain 794 consisted mainly of solitary cells or short chains formed by dividing terminal cells. Slightly convex valves exist. In most specimens, small spines are scattered over the valve surface (Fig. 3, D, E, and G). At their bases, the fultoportulae are flanked by three satellite pores. The TFPPs are open with a markedly tapered, sometimes undulate distal spine (Fig. 3, C–G and J). The IFPPs have narrow, pointed distal ends, sometimes ending in a spine (Fig. 3, G–I). The adjoining IFPPs of sibling valves are displaced and appressed sideways at their tips, the interlock being reinforced by a rectangular lateral expansion (Fig. 3, H–I). The junction is always 1:1. In strain 794, couplets of valves with FPPs leaning onto the mantle of the sibling valve were frequently observed (Fig. 3J). These were probably dividing terminal cells. The TRP lies just inside the marginal ring of TFPs and has a long process that is wider and obliquely truncated at its tip, with a spoutlike teapot end (Fig. 3, C, E, and F). The IRP is marginal and has a short process (Fig. 3G). The copulae are very delicate, with a median ridge running their entire length. The ridge is flanked on both sides by thin transverse ribs that are interspersed by hyaline areas (Fig. 3K). Valve morphology was not affected by variation in salinities from 8 to 35 psu.

Molecular analyses. SSU rDNA: The alignment used for phylogenetic analyses included 1760 positions. The ingroup contained a significant phylogenetic signal ($g_1 = -0.82$), given 93 parsimony-informative positions (threshold $g_1 = -0.12$ for 100 parsimony-informative sites and 25 sequences).

Intraspecific variation was observed among the three SSU sequences of *S. ardens*. Between positions 154 and 253, their sequences differed at 19 sites. At those sites, CCMP794 shared the same bases with sequences of all other *Skeletonema* species, CS347 possessed distinct ones, and CS348 showed ambiguities between the two. Fifteen of these 19 sites were clustered between positions

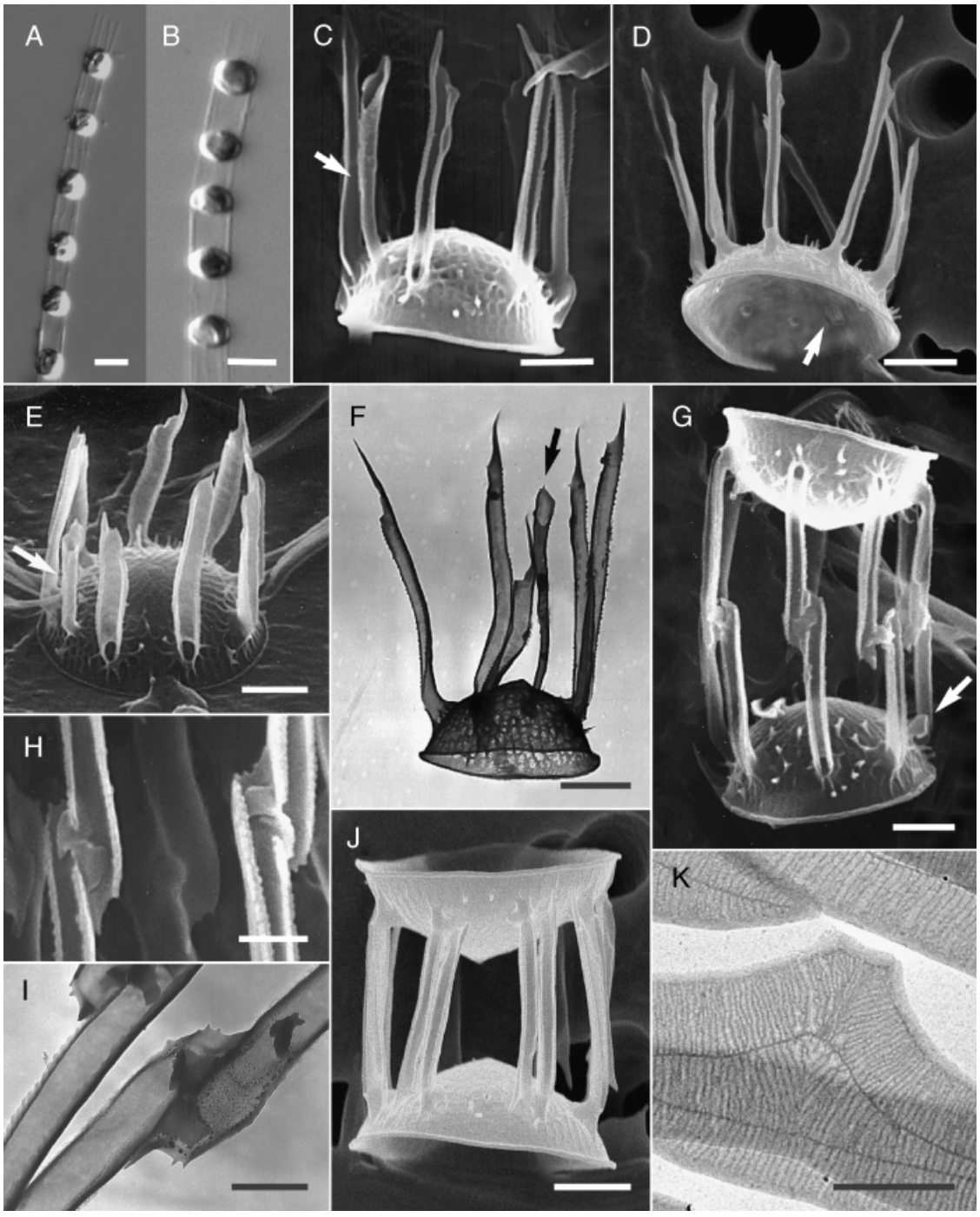

FIG. 3. *Skeletonema ardens*. LM, differential interference contrast: A and B. SEM: C–E, G, H, and J. TEM: F, I, and K. (A) Strain CS347, colony. Scale bar, 5 μm. (B) Strain CCMP794, colony. Scale bar, 5 μm. (C) Strain CS348, terminal valve showing the long marginal TRPP (arrow) with its obliquely truncated margin. Scale bar, 1 μm. (D) Strain CCMP794, terminal valve with the marginal TRP seen from the inside (arrow). Scale bar, 1 μm. (E) Strain CS348, terminal valve with the long marginal TRPP (arrow). Scale bar, 1 μm. (F) Strain CS348, terminal valve with the long marginal TRPP (arrow). Scale bar, 1 μm. (G) Strain CCMP794, intercalary valves with the IRPP (arrow). Scale bar, 1 μm. (H) Strain CS347, detail of junctions. Note the interlock reinforced by a lateral expansion. Scale bar, 0.5 μm. (I) Strain CS347, detail of a junction. Scale bar, 0.5 μm. (J) Strain CCMP794, valves in division stage. Scale bar, 1 μm. (K) Strain CS347, cingular band with thin transverse ribs interspaced by hyaline areas. Scale bar, 1 μm. IRPP, intercalary rimoportula process; LM, light microscopy; TRP, terminal rimoportula; TRPP, terminal rimoportula process.

154 and 186. This region of the SSU alignment was invariable across all other *Skeletonema* species. Beyond position 253, the three sequences were almost identical to one another. The DNA extraction, PCR amplification, and sequencing were repeated for these three strains, with the same results.

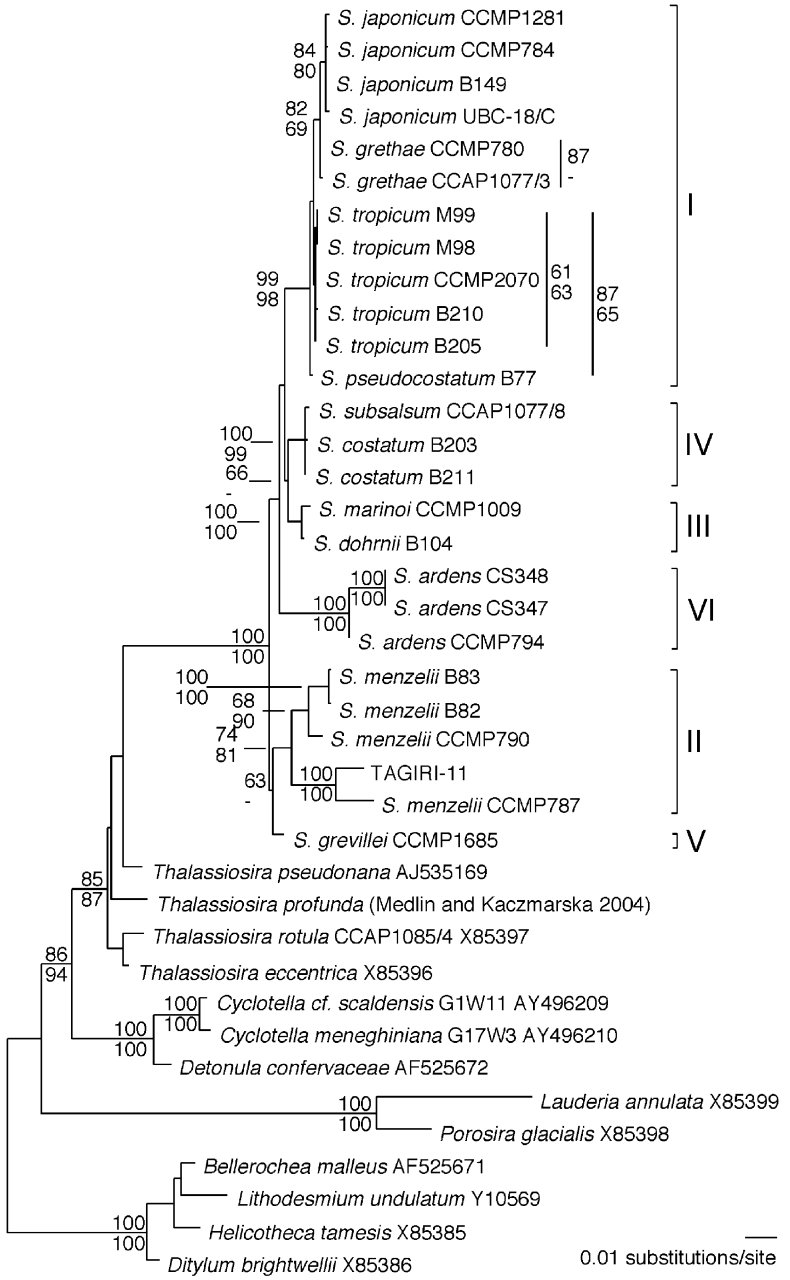

FIG. 4. One out of two equally maximum-likelihood (ML) trees inferred from the alignment of SSU rDNA sequences. Estimated parameter settings: A $\Longleftrightarrow$ C = 1.1187, A $\Longleftrightarrow$ G = 2.8531, A $\Longleftrightarrow$ T = 1.2761, C $\Longleftrightarrow$ G = 1.2705, C $\Longleftrightarrow$ T = 4.7871 relative against G $\Longleftrightarrow$ T = 1.0000; proportion of invariable sites = 0.5377; γ shape parameter = 0.8081; base frequencies: A = 0.2667, C = 0.1955, G = 0.2530, and T = 0.2848. – ln L = 7001.19136. Bootstrap values associated to clades: upper value inferred from neighbor joining (NJ), lower value from maximum parsimony (MP).

The ML analysis of the SSU alignment constrained with estimated parameter settings (legend of Fig. 4) resulted in two equally most likely trees differing only in the branching order among the *S. tropicum* sequences. One of these trees is depicted in Figure 4. Topologies of an NJ tree inferred from pair-wise ML distances, and two equally MP trees (tree statistics, Table 3) were topologically similar to the ML trees and not significantly worse, given the aforementioned substitution model (results, see Table 4). Bootstrap values calculated using MP and NJ were also similar (Fig. 4). Six lineages were recovered in *Skeletonema*: one with *S. pseudocostatum*, *S. tropicum*, *S. grethae*, and *S. japonicum* (I); one with *S. menzelii* (II); one with *S. marinoi* and *S. dohrnii* (III); one with *S. costatum* and *S. subsalsum* (IV); one with *S. grevillei* (V); and one with *S. ardens* (VI). The numbering corresponds to that in Sarno et al. (2005) for comparative reasons. The re-

TABLE 3. Tree statistics of parsimony trees with outgroups included and excluded.

Sequence	Tree length	PU	PI	RC	HI
All sequences					
SSU	869	112	330	0.621	0.325
LSU	517	45	198	0.562	0.369
Skeletonema only					
SSU	257	64	93	0.766	0.276
LSU	172	33	85	0.772	0.229

HI, homoplasy index; LSU, large subunit; PI, parsimony-informative sites; PU, parsimony-uninformative sites (autapomorphy); RC, rescaled consistency index; SSU, small subunit.

TABLE 4. Results of Shimodaira-Hasegawa test using RELL bootstrap (one-tailed test).

Trees	− ln L	Diff − ln L	*P*
SSU			
ML	7001.19136	(Best)	
NJML	7006.86416	5.67280	0.440
MP1	7006.64472	5.45336	0.400
MP2	7005.72135	4.52999	0.459
LSU			
ML	3357.46748	(Best)	
ML*	3358.03611	0.56863	0.739
NJML	3368.06100	10.59352	0.146
MP	3361.50605	4.03857	0.425

Number of bootstrap replicates = 1000.

LSU, large subunit; ML, maximum-likelihood; MP, maximum-parsimony; NJML, neighbor-joining tree of pair-wise ML distances; SSU, small subunit; RELL, resampling of estimated ln likelihood.

lationships among the six lineages remained basically unresolved. In Figure 4, *S. dohrnii*, *S. marinoi*, *S. costatum,* and *S. subsalsum* formed a clade, and so did *S. grevillei* and *S. menzelii*, although these two clades lacked firm support. The outgroups did not distort relationships among the *Skeletonema* sequences because the results of NJ-bootstrap analyses with the outgroups removed showed only improved support for grouping *S. menzelii* and *S. grevillei* (92%), whereas resolution among the other lineages was just as poor as with outgroups included. The removal of positions 154–186 (i.e., those showing the peculiar pattern among the *S. ardens* sequences) did not change the topology or improve resolution, and neither did removal of CS347 and CS348, or CCMP794 and CS348, or all three of them.

LSU rDNA: The alignment used for phylogenetic analysis included 600 positions. The ingroup contained a significant phylogenetic signal ($g_1 = -0.74$), given 85 parsimony-informative positions and 21 distinct sequences (threshold $g_1 = -0.19$ for 50 parsimony-informative sites and 15 distinct sequences).

The sequences of *S. ardens*, *S. tropicum*, *S. pseudocostatum*, and *S. menzelii* revealed conspicuous, species-specific groupings of base changes in regions where all other *Skeletonema* sequences varied little or not at all. Between positions 48 and 106, the sequences of *S. ardens* differed in 12 positions from all other *Skeletonema* sequences, and three multisite gaps had to be introduced. Between positions 135 and 173, those of *S. pseudocostatum* and *S. tropicum* differed at 14 positions from all other *Skeletonema* sequences. Between positions 189 and 210, *S. menzelii* strain CCMP787 differed from its conspecifics at 10 positions, whereas all other *Skeletonema* sequences differed in that region only in six positions.

Intraspecific variation was observed among the three LSU sequences of *S. ardens*, as in the SSU sequences. The sequences of strain CS347 and CCMP794 differed at five positions, and in four out of these five, the sequence of strain CS348 showed the expected ambiguities. Three additional positions in the latter showed ambiguities, but at those positions, the other two sequences shared identical bases. Ambiguities were also evident among the sequences of *S. subsalsum* and *S. costatum*. All sequences of *S. costatum* differed from that of *S. subsalsum* at eight positions, and four positions showed differences or ambiguities among the *S. costatum* strains.

The ML analysis of the LSU alignment constrained with estimated parameter settings (legend of Fig. 5) resulted in four equally most likely trees, of which one is depicted in Figure 5. They differed only in the branching order among the *S. costatum* sequences. Topologies of an NJ tree inferred from pair-wise ML distances, and an MP tree (statistics, see Table 3) were virtually the same as those in the ML trees, and these topologies were not significantly worse than those of the two ML trees (Table 4), given the aforementioned substitution model. Therefore, bootstrap values were calculated using MP and NJ (Fig. 5). The values obtained using the two methods were in agreement. Among the outgroup sequences, those of *Cyclotella* did not form a clade. Within *Skeletonema*, *S. subsalsum* branched off first, followed by *S. costatum*. Thus, lineage IV in the SSU tree constituted a basal grade in the LSU tree. Yet, a topology with these sequences forming a clade was not less informative (Table 4). The next to branch off was a well-supported clade with *S. grevillei* (lineage V) and *S. ardens* (lineage VI). Then followed a well-supported clade with *S. marinoi* and *S. dohrnii* (lineage III). *Skeletonema menzelii* (lineage II) branched off next, but grouping of these sequences was supported. Within the final, well-supported clade (lineage I), *S. japonicum* branched off first, followed by *S. grethae*, *S. pseudocostatum*, and *S. tropicum*. Branching patterns among all these clades within *Skeletonema* generally yielded high MP- and NJ-bootstrap support. The removal of positions 48–106, where sequences of *S. ardens* revealed high variation; positions 135–173, where those of *S. tropicum* and *S. pseudocostatum* varied radically from the remainder; and positions 189–210, where *S. menzelii* strain CCMP787 varied, did not affect branching order or bootstrap support.

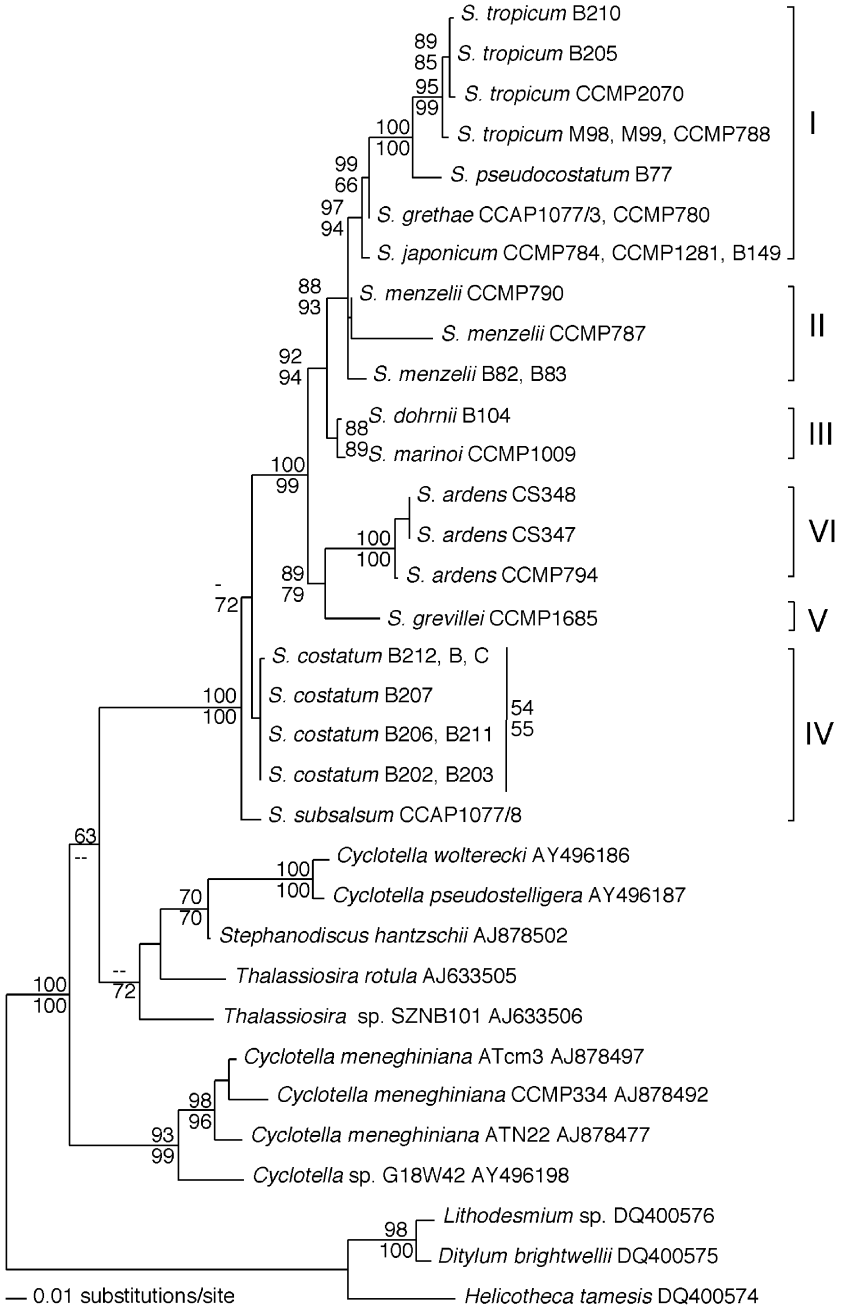

FIG. 5. Maximum-likelihood (ML) tree inferred from the alignment of partial LSU rDNA sequences. Estimated parameter settings: A $\Longleftrightarrow$ C = 0.8698, A $\Longleftrightarrow$ G = 2.5676, A $\Longleftrightarrow$ T = 2.0914, C $\Longleftrightarrow$ G = 0.6267, C $\Longleftrightarrow$ T = 5.8632 relative against G $\Longleftrightarrow$ T = 1.0000; γ shape parameter = 0.4056; and estimated base frequencies: A = 0.2327, C = 0.2037, G = 0.2980, and T = 0.2656. – ln L = 3357.46748. Bootstrap values associated to clades: upper value inferred from neighbor joining (NJ), lower value from maximum parsimony (MP).

Comparison between SSU and LSU trees. The topology within the *Skeletonema* clade in the LSU tree was well resolved, given the high bootstrap support for most ramifications, whereas that in the SSU tree lacked support for any of the deeper ramifications. The lower portion of the *Skeletonema* clade in the SSU tree was recovered in the unresolved basal polytomy, but the root taxa in the LSU tree appeared off-center, generating an oddly skewed topology, such that even morphologically similar species like *S. costatum* and *S. subsalsum* formed a grade. Apart from this, the two trees showed disagreement in the branching order of *S. japonicum* and *S. grethae*, but these species were at least recovered together in lineage I. The trees also differed in the position of *S. menzelii* (lineage II). In the SSU tree, the latter taxon was resolved as sister to *S. grevillei* (lineage V; with marginal support), whereas in the LSU tree, it appeared firmly as sister to lineage I. Moreover, in the SSU tree, lineages II (*S. dohrnii*, *S. marinoi*) and IV (*S. costatum*, *S. subsalsum*) grouped together, although with weak support, whereas in the LSU tree, this relationship was not supported.

Analyses of the LSU data set with different subsets of the outgroup taxa excluded resulted in trees topologically similar to the LSU tree in Figure 5, with the same oddly skewed structure. Analyses of the two alignments with all outgroup sequences excluded,

and with substitution models tailored exclusively to the ingroup sequences, resulted in an SSU tree with the same ill-resolved basal topology and an LSU tree with the same topology among the ingroup taxa (tree not shown) as in Figures 4 and 5, indicating that the tree topologies were not distorted as a result of a particular outgroup choice.

DISCUSSION

Skeletonema costatum. *Skeletonema* strains from the Indian River Lagoon (FL, USA), Montevideo (Uruguay), and the Lagoa dos Patos (Brazil) match type material from Hong Kong Bay. These strains also share highly similar rDNA sequences that are distinct from those of other *Skeletonema* species. All the distinctive LM and EM characters of *S. costatum* (Zingone et al. 2005) were also observed. Both type material and cultures have split processes with clawlike tips in terminal valves and flattened, closed IFPPs. A minor difference is that the IFPPs in the type material were always perfectly closed tubules fused along the entire length with barely any visible suture, whereas a suture was visible in the cultures, and the margins sometimes separated at their distal end or most of their length. This may be an effect of cultivation, possibly related to the degree of silicification.

A constant, distinctive feature is the presence of 1:2 relationships around the entire junction between sibling valves, whereas at least some 1:1 junctions are always found in other *Skeletonema* species, including *S. subsalsum* (Table 2). The marginal position of the terminal rimoportula was also confirmed in cultures. This is a rather rare feature shared only by *S. costatum*, *S. grevillei*, and *S. ardens*.

Finding live *S. costatum* strains allowed confirmation of the stability of most morphological characters that were considered important when the species was redefined (Zingone et al. 2005). The short fultoportula processes (FPPs), flattened valve faces, and high mantles at low salinities were not observed in the type material, probably because salinity in Hong Kong Bay was higher at the time of the collection, also corroborated by the typically marine microflora in those samples (Zingone et al. 2005). In a recent global survey of the genus (Kooistra et al., submitted), specimens with long FPPs were seen in EM illustrations from natural samples, suggesting that this morphology is stable in the marine environment.

Shortening of the processes at low salinities (<3 psu) is similar to that described for *S. subsalsum*, which shares the capacity to grow in salinities of ~0 psu (Hasle and Evensen 1975, Paasche et al. 1975). In contrast, *S. ardens* and *S. grevillei* cannot grow below 8 psu and do not show morphological changes at the lower part of their salinity tolerance range, nor over the rest of the salinity range tested. Other *Skeletonema* species (*S. pseudocostatum*, *S. dohrnii*, and *S. japonicum*) showed similar lack of morphological variability in parallel experiments (unpublished results). *Skeletonema costatum* and *S. subsalsum* shared other characteristics. As discussed previously (Sarno et al. 2005, Zingone et al. 2005), IFPPs often closed along their length, and 1:2 junctions clearly identify *S. subsalsum* as the sister species to *S. costatum*. Our new observations on live *S. costatum* highlight another remarkable resemblance to *S. subsalsum*: both species have girdle bands with transverse branching ribs interspersed by rows of small pores. The position of the TRP and the shape of the TFFPs are remarkably different in the two species, although it is worth noting that our observations on *S. subsalsum* are based on a single strain kept in culture since 1991, while *S. costatum* has now been observed in field material and in recently established cultures. *Skeletonema subsalsum* might show morphological variability in freshly isolated or field material.

In the light of their juxtaposition in the LSU tree and virtual SSU identity, the similar morphology and physiology of *S. costatum* and *S. subsalsum* are not surprising. The great similarity of the two species could make their separation difficult, especially in material from low-salinity waters. A revision of previous reports of *S. subsalsum* is therefore needed to evaluate the ranges of the two species.

Skeletonema grevillei. Morphological features of the strain of *S. grevillei* from the Arabian Sea match the type material (Zingone et al. 2005). Both share similar terminal and intercalary FPPs and the peculiar peripheral position of the terminal rimoportula, and both have silica ridges at the bases of the FPP, although there are differences in the extent of these structures. The ridges connecting the internal faces of the bases of the FPPs, and those that join the lateral faces of the bases of the FPPs, were generally present in the Arabian Sea strain, but they were often incomplete. The ridges delimiting an external hole at the base of each FPP in a few specimens of the type material (fig. 6F in Zingone et al. 2005) were never observed in cultured material. But variability in the extent and complexity of the ridges was evident among specimens in the original material (cf. fig. 6 in Zingone et al. 2005), ridge reduction being more noticeable in smaller cells (<4 μm) as in the Arabian Sea strain (fig. 6, A and C in Zingone et al. 2005). Sarno et al. (2005) noted a similarity in process shape and junctions between *S. grethae* and *S. grevillei*, but the marginal position of the TRP in *S. grevillei* rather supports the closer relationship with *S. ardens* shown by the phylogenetic tree.

Skeletonema ardens. This species shares the marginal position of the rimoportula in the terminal valve with *S. costatum* and *S. grevillei*, a character found only in these three species (Table 2). The shape of the IFFPs (open along their entire length) and their connection mode (1:1) clearly separates *S. ardens* from *S. costatum*, while the peculiar flamelike edges of the terminal processes differentiate it from both *S. costatum* and *S. grevillei*. In contrast, *S. ardens* and *S. grevillei* share a number of characters, includ-

ing the shape of the junctions between IFPPs of sibling valves, which are slightly displaced and laterally interlocked, and the remarkably delicate copulae.

With respect to other *Skeletonema* species, *S. ardens* shares narrow processes, never widening at their tips, with two taxa in lineage I: *S. grethae* and *S. pseudocostatum* (Sarno et al. 2005). The small spines scattered over the valve surface, typical of all *S. ardens* strains, were occasionally observed in the single-celled *S. menzelii*, but not in any colonial *Skeletonema* species (Sarno et al. 2005). Morphological differences among the strains of *S. ardens* (e.g., in colony formation) cannot be evaluated properly because only cultured material (grown for 15–30 years) was examined. Long-term cultures of many diatoms tend to become morphologically atypical.

The genetic variation within *S. ardens* is comparable to that observed between genotypes within other morphologically delineated species, such as *S. menzelii*, or among genotypes of morphologically similar species (e.g., *S. marinoi* and *S. dohrnii*). In the case of *S. ardens*, we retain all the genotypes under the same name, because the small number of strains does not allow us to assess whether the differences represent intraspecific variation, cryptic, or pseudocryptic species. In the case of *S. dohrnii*/*S. marinoi*, we separated the taxa because they showed subtle morphological differences and because they were found in sympatry at least once. A recent extensive biogeographic study of the genus (Kooistra et al., submitted) has revealed molecular diversity in other *Skeletonema* species, namely *S. tropicum* and *S. pseudocostatum*, as well as separation of *S. dohrnii* into at least four LSU genotypes. In all these cases, additional morphological and population genetics research is needed before sequence differences are accorded taxonomic significance.

Phylogeny. The contrasting topologies of the SSU and LSU trees suggest a conflict between the phylogenetic information in these two markers. However, the LSU tree is better resolved, and in those cases where the SSU topology conflicts with the LSU topology, the SSU arrangements show low (if any) bootstrap support. Whether the well-resolved LSU tree accurately reflects *Skeletonema* evolution remains to be tested with other markers. In any case, the off-center root to the tree is not due to poor outgroup choice, because the removal of various sets of outgroup sequences results in the same skew.

Addition of the *S. ardens*, *S. costatum*, and *S. grevillei* sequences did not alter relationships among the other species; the tree topologies in this study corroborate those in Sarno et al. (2005) and Alverson and Kolnick (2005). In addition, the phylogenetic position of *S. tropicum* near *S. pseudocostatum* in the SSU tree is in accordance with its position in our LSU trees and those in Sarno et al. (2005). The presence of an insert in the 3′- (reverse) primer explains why the latter failed to sequence the SSU of the Mediterranean strains of this species. The other SSU types within *S. tropicum* lack this insert and are PCR-amplified without trouble.

Extended branch lengths in the lineages of *S. ardens* in the SSU tree; of *S. ardens*, *S. grevillei*, and *S. menzelii* CCMP787; and of the *S. tropicum* and *S. pseudocostatum* clade result from clusters of base changes in sequence regions where other *Skeletonema*, and often even outgroups, show little, if any, change. These peculiar patterns might constitute scars from mobile genetic elements, such as class II transposons (Kidwell 2005) and other temporal insertions, such as that present in the SSU of the Neapolitan strains of *S. tropicum*. The long branches do not result from elevated substitution rates over the entire sequences of these species because exclusion of the scarred positions results in trees with identical topology but without long branches.

All morphologically defined taxa in this study and in Sarno et al. (2005) constitute monophyletic entities, or their monophyly cannot be rejected (*S. grethae*, *S. costatum*, and *S. menzelii*). However, in the sense that both their LSU and SSU sequences group in two or more clades, these morphological taxa sometimes include cryptic species. Sarno et al. (2005) and Kooistra et al. (submitted) identified three genetically distinct lineages in *S. menzelii*. That a sequence of environmental clone TAGIRI-11 also groups within this clade indicates the existence of yet another cryptic species in *S. menzelii*, although we lack morphological data to confirm the genetic identification. The fact that this material was sampled from anoxic sediment around fumaroles on a submarine caldera floor (Takishita et al. 2005) suggests that the sequence originated from a recently deposited zooplankton fecal pellet or a resting stage, and that the cell was viable. Paraphyly for *S. grethae* in an SSU tree (Alverson and Kolnick 2005) is probably due to the misnaming of strain UBC 18/C by Sarno et al. (2005). The latter labeled this strain as *S. grethae*, but it groups with the remaining strains of *S. japonicum* (Kooistra et al., submitted). It has not been examined morphologically.

Phylogenetic value of morphological characters revisited. The results of this study confirm that the shape of FPPs is lineage-specific (Sarno et al. 2005), and that process morphology and mode of interlocking tend to be constant within lineages. In *S. costatum* and *S. subsalsum* (lineage IV), the IFPPs are generally closed tubules with a longitudinal suture that may be partially open. In *S. grevillei* and *S. ardens* (lineages V and VI), FPPs always have narrow ends and lateral junctions. Lineage III (*S. dohrnii* and *S. marinoi*) is also homogeneous, all FPPs have wider distal portions, and IFPPs have plain joints. Lineage II comprises a single, noncolonial species, *S. menzelii*, with narrow, spiny-ended processes. Lineage I is more heterogeneous, FPP ends being narrow in the 1:1 mode, but wide in 1:2 junctions encountered in *S. japonicum* and *S. tropicum*. Within this clade, junctions are generally knot- or knuckle-shaped. Despite the relative consistency of FPP shape within clades, the relationships between the different clades with respect to this character are unclear; it seems that the shape of these processes has changed several times.

Terminal rimoportula position varies in accordance with tree topology. In species belonging to lineages I, II, and III, it is central or subcentral; but it is marginal in those of lineages IV, V, and VI, with the exception of *S. subsalsum*, where it is subcentral. The most parsimonious explanation for the evolution of this character is that the process moved from the margin toward the valve center in *S. subsalsum*, independent of a similar change in the last common ancestor of lineages I, II, and III. It is difficult to predict the position of the rimoportula in the common ancestor of the genus; yet, it should be noted that rimoportula position varies considerably within the Thalassiosirales, although it is more frequent at the valve margin (Kaczmarska et al. 2005). While differing in the position of their terminal rimoportulae, *S. costatum* and *S. subsalsum* both have long intercalary rimoportula processes, a feature confined to these two.

CONCLUSION

Skeletonema ardens, *S. costatum*, and *S. grevillei* are morphologically and genetically distinct, and molecular results corroborate the taxonomic relevance of the morphological features considered unique for these species (Zingone et al. 2005) and separate them from other *Skeletonema* species (Sarno et al. 2005). The diagnostic value of most characters demarcating *Skeletonema* species has also been validated (Sarno et al. 2005), reaffirming the importance of microanatomical observations in marine phytoplankton systematics.

Molecular results have demonstrated the phylogenetic relatedness of *S. costatum* and *S. subsalsum*, which had been hypothesized from their morphological similarity (Sarno et al. 2005). This finding is matched by their tolerance to low salinities (close to 0 psu), where they show a similar, unique morphological response, namely the reduction in the length of FPPs. *Skeletonema grevillei* and *S. ardens* form a separate lineage and are not closely related to species of clade I, with whom they share narrow FPPs and knucklelike IFPP junctions, but not a marginal TRP. Fultoportulae have presumably changed shape several times, whereas rimoportula position has changed only twice. Nevertheless, both characters are important for taxon identification.

Skeletonema ardens, *S. costatum*, and *S. grevillei* were collected during the course of a global survey of *Skeletonema* species (Kooistra et al., submitted), although absent from our earlier collection (Sarno et al. 2005), which mainly consisted of strains from temperate regions. *Skeletonema ardens*, *S. costatum*, and *S. grevillei* were obtained from tropical and subtropical samples, as was the Hong Kong sample from which *S. costatum* and *S. grevillei* were first described. These areas have been less intensively investigated than temperate coastal zones. Moreover, tropical plankton diversity has been forced into "temperate" taxonomy, because many species were originally described from Europe, North America, Japan, or Australia. Thus, while knowledge of *Skeletonema* diversity in temperate areas appears to be covered by recent research (Godhe et al. 2006, Kooistra et al., submitted), the tropics might still harbor undiscovered *Skeletonema* species.

Both temperate and tropical areas are linked by genetic diversity within morphologically circumscribed taxa (this study, Godhe et al. 2006, Kooistra et al., submitted). Whether this diversity is truly cryptic should be tested with additional morphological analyses (e.g., other ultrastructural characters) or other technologies. Even if such diversity is shown to be cryptic, its origin and significance for the biogeography, ecology, and biology of diatom species warrant investigation.

We thank Gandi Forlani for his help in EM preparations, Gennaro Iamunno and Francesco Iamunno for their skillful assistance with TEM and SEM, Carmen Minucci for culture maintenance, and Elio Biffali and the staff of the molecular biology service at SZN for sequencing and other services. Marli Bergesch kindly provided strains from Brazil, and Silvia Méndez graciously collected a net sample from Uruguay. Haifeng Gu is gratefully acknowledged for sending the strain SCXM09, from which Figure 1A was taken. The molecular and morphological research has entirely been funded by SZN. P. E. H. was partially supported by the Smithsonian Marine Station, Fort Pierce, FL, USA, contribution #660 from SMS. The present study is a contribution to the EU Network of Excellence MARBEF, Marine Biodiversity and Ecosystem Functioning.

Alverson, A. J. & Kolnick, L. 2005. Intragenomic nucleotide polymorphism among small subunit (18S) rDNA paralogs in the diatom genus *Skeletonema* (Bacillariophyta). *J. Phycol.* 41:1248–57.

Anonymous, X. 1975. Proposals for a standardization of diatom terminology and diagnoses. *Nova Hedwigia Beih.* 53:323–54.

Bethge, H. 1928. Über die Kieselalge *Skeletonema subsalsum* (A. Cleve) Bethge. *Ber. dt. bot. Ges.* 46:340–7.

Cleve, P. T. 1900. Notes on some Atlantic plankton-organisms. *Kongl. Svensk Vetensk.-Akad. Handl.* 34:3–22.

Corpet, F. 1998. Multiple sequence alignment with hierarchical clustering. *Nucleic Acids Res.* 16:10881–90.

Godhe, A., McQuoid, M. R., Karunasagar, I., Karunasagar, I. & Rehnstam-Holm, A.-S. 2006. Comparison of three common molecular tools for distinguishing among geographically separated clones of the diatom *Skeletonema marinoi* Sarno et Zingone (Bacillariophyceae). *J. Phycol.* 42:280–91.

Greville, R. K. 1866. Description of new and rare diatoms. Series 20. *Trans. Microsc. Soc. London n. s.* 14:77–86.

Guillard, R. R. L., Carpenter, E. J. & Reimann, B. E. F. 1974. *Skeletonema menzelii* sp. nov., a new diatom from the western Atlantic Ocean. *Phycologia* 13:131–8.

Hasle, G. R. 1978. Diatoms. *In* Sournia, A. [Ed.] *Phytoplankton Manual*. UNESCO, Paris, pp. 136–42.

Hasle, G. R. & Evensen, D. L. 1975. Brackish-water and fresh-water species of the diatom genus *Skeletonema* Grev. I. *Skeletonema subsalsum* (A. Cleve) Bethge. *Phycologia* 14:283–97.

Hillis, D. M. & Huelsenbeck, J. P. 1992. Signal, noise, and reliability in molecular phylogenetic analyses. *J. Hered.* 83:189–95.

Kaczmarska, I., Beaton, M., Benoit, A. C. & Medlin, L. K. 2005. Molecular phylogeny of selected members of the order Thalassiosirales (Bacillariophyta) and evolution of the fultoportula. *J. Phycol.* 42:121–38.

Kidwell, M. G. 2005. Transposable elements. *In* Gregory, T. R. [Ed.] *The Evolution of the Genome*. Elsevier, San Diego, CA, USA, pp. 165–221.

Kooistra, W. H. C. F., DeStefano, M., Mann, D. G., Salma, N. & Medlin, L. K. 2003. The phylogenetic position of *Toxarium*, a

pennate-like lineage within centric diatoms (Bacillariophyceae). *J. Phycol.* 39:185–97.

Medlin, L. K., Elwood, H. J., Stickel, S. & Sogin, M. L. 1991. Morphological and genetic variation within the diatom *Skeletonema costatum* (Bacillariophyta): evidence for a new species, *Skeletonema pseudocostatum*. *J. Phycol.* 27:514–24.

Medlin, L. K. & Kaczmarska, I. 2004. Evolution of the diatoms: V. morphological and cytological support for the major clades and a taxonomic revision. *Phycologia* 43:245–70.

Orsini, L., Sarno, D., Procaccini, G., Poletti, R., Dahlmann, J. & Montresor, M. 2002. Toxic *Pseudo-nitzschia multistriata* (Bacillariophyceae) from the Gulf of Naples: morphology, toxin analysis and phylogenetic relationships with other *Pseudo-nitzschia* species. *Eur. J. Phycol.* 37:247–57.

Paasche, E., Johansson, S. & Evensen, D. L. 1975. An effect of osmotic pressure on the valve morphology of the diatom *Skeletonema subsalsum*. *Phycologia* 14:205–11.

Rambaut, A. 1996-2002 Sequence Alignment Editor v2.0a11. http://evolve.zoo.ox.ac.uk/ (accessed 18/01/05).

Ross, R., Cox, E. J., Karayeva, N. I., Mann, D. G., Paddock, T. B. B., Simonsen, R. & Sims, P. A. 1979. An amended terminology for the siliceous components of the diatom cell. *Nova Hedwigia Beih.* 64:513–33.

Sarno, D., Kooistra, W. C. H. F., Medlin, L. K., Percopo, I. & Zingone, A. 2005. Diversity in the genus *Skeletonema* (Bacillariophyceae). II. An assessment of the taxonomy *S. costatum*-like species, with the description of four new species. *J. Phycol.* 41:151–76.

Swofford, D. L. 2002. *PAUP*: Phylogenetic Analysis Using Parsimony (* and Other Methods). Version 4.0b10*. Sinauer Associates, Sunderland, MA, USA.

Takishita, K., Miyake, H. & Kawato, M. 2005. Genetic diversity of microbial eukaryotes in anoxic sediment around fumaroles on a submarine caldera floor based on the small-subunit rDNA phylogeny. *Extremophiles* 9:185–96.

Zingone, A., Percopo, I., Sims, P. A. & Sarno, D. 2005. Diversity in the genus *Skeletonema* (Bacillariophyceae). I. A re-examination of the type material of *Skeletonema costatum*, with the description of *S. grevillei* sp. nov. *J. Phycol.* 41:140–50.